SCIENTIFIC REPORTS

OPEN

Dual effect of PEG-PE micelle over the oligomerization and fibrillation of human islet amyloid polypeptide

Received: 10 August 2017
Accepted: 7 February 2018
Published online: 13 March 2018

Xiaocui Fang[1], Maryam Yousaf[1,2], Qunxing Huang[1], Yanlian Yang[1] & Chen Wang[1]

The oligomerization and fibrillation of human islet amyloid polypeptide (hIAPP) play a central role in the pathogenesis of type 2 diabetes. Strategies for remodelling the formation of hIAPP oligomers and fibrils have promising application potential in type 2 diabetes therapy. Herein, we demonstrated that PEG-PE micelle could inhibit hIAPP oligomerization and fibrillation through blocking the hydrophobic interaction and the conformational change from random coil to β-sheet structures of hIAPP. In addition, we also found that PEG-PE micelle could remodel the preformed hIAPP fibrils allowing the formation of short fibrils and co-aggregates. Taken together, PEG-PE micelle could rescue hIAPP-induced cytotoxicity by decreasing the content of hIAPP oligomers and fibrils that are related to the oxidative stress and cell membrane permeability. This study could be beneficial for the design and development of antiamyloidogenic agents.

The deposition of insoluble amyloid aggregates, formed due to misfolding of proteins and peptides, is involved in the pathogenesis of many amyloidogenic diseases including Parkinson's disease (PD), Huntington's disease (HD), Alzheimer's disease (AD), mad cow disease, and type 2 diabetes (T2DM)[1–3]. The aggregation of human islet amyloid polypeptide (hIAPP) is one of the common representative examples because of its rapid aggregation dynamics. hIAPP is a 37-residue peptide synthesized and co-secreted along with insulin in pancreatic β-cells[4]. hIAPP shows the propensity to aggregate from its normally soluble and functional states into insoluble and β-sheet-rich amyloid[5–7]. hIAPP aggregates are the main component of pancreatic amyloid deposits, one of the characteristic pathological features of T2DM[5,8,9]. Extensive studies have shown that the deposition of hIAPP amyloid is associated with pancreatic β-cell dysfunction and loss of β-cell mass, which is the main cause of T2DM pathogenesis[6,10]. In this regard, inhibitors targeting hIAPP aggregates hold great application potential.

Although hIAPP adopts various conformations *i.e.*, from monomer, dimer and soluble oligomer to protofibril and fibril during its aggregation process, it has been generally accepted that amyloid oligomers have greater toxicity compared to monomers or fibrils. Early hIAPP inhibitors have focused on the insoluble fibrils as they were thought to be the primary pathogenic species due to their prevalence in the pancreatic amyloid deposits[9]. A number of inhibitors, such as peptides[11], coordination compounds[12,13], small molecules[14], nanoparticles[15], dendritic polymers[16,17] and macromolecules[18], have been developed to bind with hIAPP and to remodel its assembly. These molecular binding agents have been shown to disrupt the fibrillation of hIAPP and to rescue hIAPP-induced cytotoxicity. In recent years, the attention has been shifted towards the early stage of hIAPP fibrillation *i.e.*, soluble oligomers and protofibrils as they were suggested to be the primary toxic species involved in β-cell dysfunction and cell death in T2DM. However, none of the hIAPP commercial inhibitor has been approved clinically for T2DM therapy, due to the efficiency of these inhibitors usually vary from case to case and is also condition-dependent. The current clinical treatment for T2DM is a continuous subcutaneous insulin infusion, but the repeated insulin injection in the same site can cause local reactions of subcutaneous scleroma, fat atrophy and ache, which limits its widespread application. Therefore, it is highly desirable to develop more effective candidates for hIAPP inhibitors.

PEG-PE molecule consists of hydrophilic polyethylene glycol (PEG) and hydrophobic phosphatidylethanolamine (PE). The polymeric micelle comprised of amphiphilic PEG-PE molecules is a promising nano-sized system

[1]CAS Key Laboratory of Standardization and Measurement for Nanotechnology, CAS Key Laboratory of Biological Effects of Nanomaterials and Nanosafety, CAS Center for Excellence in Nanoscience, National Center for Nanoscience and Technology, Beijing, 100190, P. R. China. [2]Radiation Chemistry Laboratory, Department of Chemistry, University of Agriculture, Faisalabad, 38000, Pakistan. Correspondence and requests for materials should be addressed to Y.Y. (email: yangyl@nanoctr.cn) or C.W. (email: wangch@nanoctr.cn)

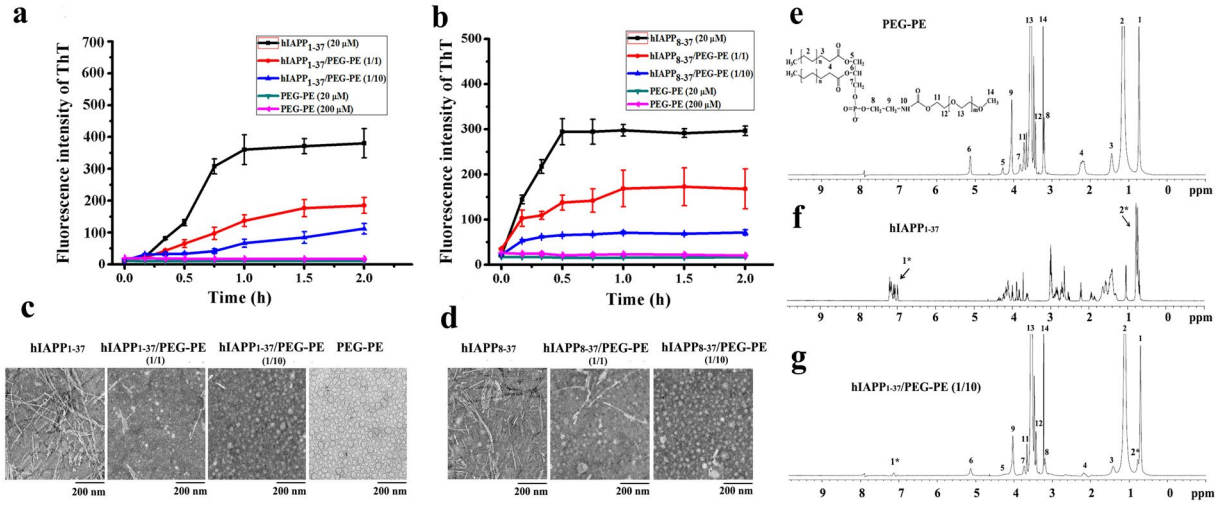

Figure 1. Antiamyloidogenic effect of PEG-PE micelles on $hIAPP_{1-37}$ and $hIAPP_{8-37}$. (**a**,**b**) The representative plots showing the kinetics of (**a**) $hIAPP_{1-37}$ and (**b**) $hIAPP_{8-37}$ aggregation in the absence and presence of PEG-PE micelles. 20 μM solutions of $hIAPP_{1-37}$ and $hIAPP_{8-37}$ were incubated at 37 °C for 2 h with and without PEG-PE micelles at various PEG-PE/hIAPP molar ratios: 1:1 (20 μM/20 μM) and 10:1 (200 μM/20 μM). Error bars represent the standard deviation ($n = 3$). (**c**,**d**) TEM images of (**c**) $hIAPP_{1-37}$ and (**d**) $hIAPP_{8-37}$ after 24 h of incubation at 37 °C in the absence and presence of one and tenfold excess of PEG-PE micelles. The concentrations of $hIAPP_{1-37}$ and $hIAPP_{8-37}$ were 20 μM. (**e**,**f**,**g**) ^{1}H-NMR spectra of (**e**) PEG-PE copolymer (5 mM), (**f**) $hIAPP_{1-37}$ (0.5 mM) and (**g**) $hIAPP_{1-37}$/PEG-PE (PEG-PE:$hIAPP_{1-37}$ = 10:1, molar ratio) in D_2O.

for both chemotherapeutic drugs and peptides because of their good biocompatibility and safety[19–23]. Our previous studies have demonstrated that PEG-PE micelle could assist non-native insulin refolding into its native states and inhibit insulin aggregation through blocking hydrophobic interactions of dithiothreitol (DTT)-denatured insulin A and B chains[20]. This prompted us whether PEG-PE micelle could remodel hIAPP assembly and rescue hIAPP-induced cytotoxicity.

Herein, we chose two hIAPP peptides ($hIAPP_{1-37}$ and $hIAPP_{8-37}$) and investigated the inhibitory effect of PEG-PE micelle on both $hIAPP_{1-37}$ and $hIAPP_{8-37}$ aggregation. These results demonstrated that PEG-PE micelle not only inhibited the oligomerization and fibrillation of $hIAPP_{1-37}$ and $hIAPP_{8-37}$, but also rescued $hIAPP_{1-37}$- and $hIAPP_{8-37}$-mediated β-cell death. We further investigated the mechanism underlying the alleviated cytotoxicity by PEG-PE micelle, and found that PEG-PE micelle reduced $hIAPP_{1-37}$- and $hIAPP_{8-37}$-induced intracellular oxidative stress and cell membrane permeability. In addition, we also evaluated the inhibitory effect of PEG-PE micelle over the preformed $hIAPP_{1-37}$ and $hIAPP_{8-37}$ fibrils, and found that PEG-PE micelle could rescue $hIAPP_{1-37}$ and $hIAPP_{8-37}$ fibrils-induced cytotoxicity through remodelling the entangled long fibrils into short fibrils and co-aggregates. This work will broaden the application of PEG-PE as an antiamyloidogenic agent.

Results

The inhibitory effect of PEG-PE micelle on $hIAPP_{1-37}$ and $hIAPP_{8-37}$ fibrillogenesis. ThT binding assay is a widely used method for monitoring amyloid aggregation[24]. ThT can generate a new fluorescence excitation maximum at 450 nm and an enhanced emission at 482 nm upon binding with β-sheet structures of amyloid aggregates. To determine whether PEG-PE micelle can act as an inhibitor for both $hIAPP_{1-37}$ and $hIAPP_{8-37}$ aggregation, the aggregation kinetics of $hIAPP_{1-37}$ and $hIAPP_{8-37}$ were monitored by measuring ThT fluorescence intensity. The freshly prepared solutions of $hIAPP_{1-37}$ and $hIAPP_{8-37}$ were incubated in the absence and presence of PEG-PE micelles at different molar ratios (hIAPP:PEG-PE molar ratio was varied from 1:0 to 1:10), and the fluorescence emission of ThT was followed for 2 h. The relative ThT fluorescence intensity was plotted as a function of time. As shown in Fig. 1a, in the absence of PEG-PE micelles, the ThT fluorescence of $hIAPP_{1-37}$ gradually increased after a lag phase of ≈15 min until it reached a plateau at ≈60 min, exhibiting a characteristic quasi-sigmoidal shape. Meanwhile, the ThT fluorescence of $hIAPP_{8-37}$ reached a plateau at ≈30 min, implying that all of the $hIAPP_{8-37}$ ended up in the form of β-sheet-rich amyloid (Fig. 1b). These results of ThT binding assay indicated that the aggregation of both $hIAPP_{1-37}$ and $hIAPP_{8-37}$ were consistent with a typical nucleation-growth mode[25]. In the presence of PEG-PE micelles, we first checked the ThT fluorescence of PEG-PE micelles alone (20 μM and 200 μM), and the result clearly demonstrated that the PEG-PE micelle didn't react with ThT molecules (Fig. 1a,b). The ThT fluorescence of both $hIAPP_{1-37}$ and $hIAPP_{8-37}$ significantly decreased to ≈50% at 1:1 molar ratio of hIAPP:PEG-PE, and to ≈20% at 1:10 molar ratio of hIAPP:PEG-PE (Fig. 1a,b). The inhibitory effect of PEG-PE micelles on $hIAPP_{1-37}$ and $hIAPP_{8-37}$ aggregation was dose-dependent, indicated from the decreased ThT fluorescence with increasing concentrations of PEG-PE micelles. These results confirmed the strong suppression effect of PEG-PE micelles on both $hIAPP_{1-37}$ and $hIAPP_{8-37}$ fibrillogenesis.

To further verify the antiamyloidogenic activity of PEG-PE micelles on $hIAPP_{1-37}$ and $hIAPP_{8-37}$ aggregation, transmission electron microscope (TEM) was employed to detect the morphology of both $hIAPP_{1-37}$ and

$hIAPP_{8-37}$ in the absence and presence of PEG-PE micelles. We found that, in the absence of PEG-PE micelles, both $hIAPP_{1-37}$ and $hIAPP_{8-37}$ formed typical mature fibrils with a length of several micrometers after 24 h of incubation at 37 °C (Fig. 1c,d). This observation was consistent with the previous reported studies that hIAPP can gradually self-assemble into larger aggregates, including oligomers and protofibrils, and finally form mature fibrils[26–29]. In the presence of PEG-PE micelles, the formation of mature fibrils of $hIAPP_{1-37}$ and $hIAPP_{8-37}$ was greatly inhibited when the molar ratios of PEG-PE/hIAPP were increased from 1/1 to 10/1 (Fig. 1c,d). When the molar ratio of PEG-PE to hIAPP was 10, $hIAPP_{1-37}$ and $hIAPP_{8-37}$ fibrils were completely replaced by spherical particles that were very similar to the morphology of empty PEG-PE micelles (Fig. 1c). TEM results demonstrated that PEG-PE micelles could effectively inhibit the aggregation of both $hIAPP_{1-37}$ and $hIAPP_{8-37}$, in accordance with the results from ThT binding assay.

To detect in detail the interactions of hIAPP and PEG-PE, we performed the nuclear magnetic resonance (NMR) experiments. We first characterized the physical state and the chemical composition of PEG-PE using ^{1}H-NMR spectra. The concentration of PEG-PE (5 mM) in the NMR samples in this study was much higher than the critical micelle concentration (CMC) of PEG-PE in water (10 μM)[19], which imply that all of PEG-PE molecules in the samples are in a form of the micelle. The assigned proton resonances for chemical groups of PEG-PE were indicated in Fig. 1e. The signals of protons in 11-CH_2, 12-CH_2O, 13-CH_2O and 14-CH_3O of PEG chains were much narrower than those in 1-CH_3, 2-CH_2, 3-CH_2, and 4-CH_2 of PE chains. These results indicated that, in PEG-PE micelle, PEG chains have higher mobility than PE chains. Thus, the extended PEG chains form a hydrophilic outer shell, while the hydrophobic PE chains form a hydrophobic inner core in aqueous media. $hIAPP_{1-37}$ showed intrinsic specific peaks at 0.5–7.5 ppm (Fig. 1f). As shown in Fig. 1g, the ^{1}H-NMR spectrum of $hIAPP_{1-37}$/PEG-PE at 1:10 molar ratio of hIAPP:PEG-PE in D_2O also suggested the formation of the core-shell structure in comparison to the ^{1}H-NMR spectrum of empty PEG-PE micelles (Fig. 1e). However, in the presence of PEG-PE micelles, the majority of specific peaks of $hIAPP_{1-37}$ molecules at 1.0–4.5 ppm disappeared, and only the specific peaks at 7.0–7.2 ppm (black arrow 1*) and 0.6–0.9 ppm (black arrow 2*) still retained (Fig. 1g). Compared with $hIAPP_{1-37}$, the resonances of $hIAPP_{1-37}$ in the presence of PEG-PE micelles were significantly reduced and showed lower peaks that close to the baseline because of the decreased molecular motion of $hIAPP_{1-37}$ encapsulated in the micelles. Therefore, the NMR results prove that hIAPP could be intercalated into PEG-PE micelles.

In addition, dynamic light scattering (DLS) was also employed to detect the particle size distribution of $hIAPP_{1-37}$ and $hIAPP_{8-37}$ aggregates in the absence and presence of PEG-PE micelles. These results clearly showed that the average diameters of $hIAPP_{1-37}$ and $hIAPP_{8-37}$ aggregates were 4.8 μm and 2.7 μm after 24 h of incubation at 37 °C, indicating the formation of hIAPP fibrils (Supplementary Figure S1a,b). However, after addition of PEG-PE, bimodal heterogeneous distribution was observed at a molar ratio of 1:1 (PEG-PE:hIAPP) as shown in Figure S1c, d. For $hIAPP_{1-37}$/PEG-PE system, 93% of the particles have an average diameter of 28.9 nm ± 5.9 nm and 7% of the particles have an average diameter of 4.3 μm ± 1.5 μm) (Supplementary Figure S1c). The larger particles with diameter of about 4 μm could be the hIAPP aggregates. Similarly, for $hIAPP_{8-37}$/PEG-PE system, 85% of the particles have an average diameter of 22.8 nm ± 6.0 nm and 15% of the particles have an average diameter of 0.9 μm ± 0.6 μm (Supplementary Figure S1d). Moreover, the particle size distribution was more homogenous and stable with a single peak at 19.8 nm ± 4.1 nm and 19.0 nm ± 4.2 nm at a molar ratio of 1:10 (hIAPP:PEG-PE) (Supplementary Figure S1e,f). These results indicated that the ability of PEG-PE micelles to attenuate hIAPP aggregation could also manifest in reduction of hIAPP aggregates size. The particle size of PEG-PE micelle alone is about 15.9 nm ± 3.8 nm and the increased particle size for PEG-PE/hIAPP system could be ascribed to the formation of hIAPP/PEG-PE complexes (Supplementary Figure S1g).

PEG-PE micelle-induced conformational changes of $hIAPP_{1-37}$ and $hIAPP_{8-37}$. hIAPP aggregation is usually accompanied by a conformational change from the non-pathogenic random coils to the pathogenic β-sheet-rich structures[5]. To investigate the effect of PEG-PE micelles on the conformational change of hIAPP, we performed circular dichroism (CD) spectroscopy with $hIAPP_{1-37}$ and $hIAPP_{8-37}$ which were incubated in the absence and presence of one and tenfold excess concentrations of PEG-PE micelles for 20 min, 2 h and 24 h. As the introduction of PEG-PE micelles didn't cause the conformational changes compared with PBS or ddH_2O, the CD spectra of samples were measured on the baseline of PEG-PE micelles with identical concentration and incubation time. Within 2 h of incubation at 37 °C, both $hIAPP_{1-37}$ and $hIAPP_{8-37}$ in the absence of PEG-PE micelles retained their native random coil conformation with a negative band around 199 nm (Fig. 2a,b). After 24 h of incubation, both $hIAPP_{1-37}$ and $hIAPP_{8-37}$ exhibited a spectrum with a positive peak at around 195 nm and a negative peak at around 217 nm, characteristic of a β-sheet-rich structure (Fig. 2a,b). However, influenced by PEG-PE micelles, the ellipticity of the characteristic peak of β-sheet structures of both $hIAPP_{1-37}$ and $hIAPP_{8-37}$ decreased at 195 nm and increased at 208 nm and 222 nm in a dose-dependent manner (Fig. 2a,b). In addition, the proportions of secondary structures elements of $hIAPP_{1-37}$ and $hIAPP_{8-37}$ in the absence and presence of PEG-PE micelles were analyzed after 24 h of incubation at 37 °C. Compared with $hIAPP_{1-37}$, PEG-PE micelles significantly altered the relative proportions of the secondary structure elements of $hIAPP_{1-37}$ at a molar ratio of 10:1 (PEG-PE:$hIAPP_{1-37}$): β-sheet contents decreased from 72.5% to 26.1%, α-helix contents increased from 0% to 32.8%, and random coil contents increased from 5.9% to 31.9%, respectively (Supplementary Table S1). Meanwhile, the relative proportions of secondary structure elements of $hIAPP_{8-37}$ were also changed in the presence of tenfold excess concentration of PEG-PE micelles for 24 h as compared to $hIAPP_{8-37}$ alone: β-sheet contents decreased from 61.4% to 31.2%, α-helix contents increased from 0% to 30.9%, and random coil contents increased from 0% to 29.2%, respectively (Supplementary Table S2). The CD results suggested that PEG-PE micelles induced a decrease in the content of β-sheet structures and an increase in the contents of α-helical and random coil structures of both $hIAPP_{1-37}$ and $hIAPP_{8-37}$, which supported the results from ThT binding assay. Since increased β-sheet constituent is the main cause of hIAPP aggregation[25], PEG-PE micelles could hinder the

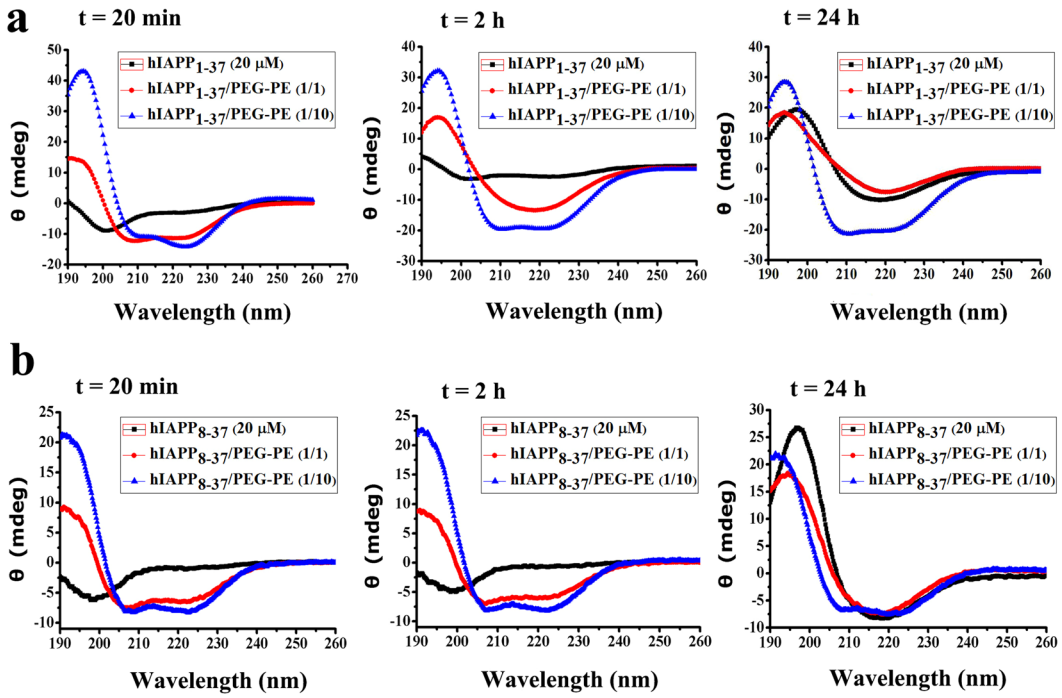

Figure 2. Circular dichroism spectra showing PEG-PE micelles inhibited conformational changes of $hIAPP_{1-37}$ and $hIAPP_{8-37}$. 20 μM solutions of (**a**) $hIAPP_{1-37}$ and (**b**) $hIAPP_{8-37}$ were incubated at 37 °C in the absence and presence of one and tenfold excess of PEG-PE micelles and analyzed after 20 min, 2 h and 24 h. The spectra represent the average of six scans after subtracting the contribution of the PEG-PE micelles at identical concentrations.

conformational transition of $hIAPP_{1-37}$ and $hIAPP_{8-37}$ from random coil to β-sheet, which eventually inhibited the fibrils formation of $hIAPP_{1-37}$ and $hIAPP_{8-37}$.

The inhibitory effect of PEG-PE micelles on $hIAPP_{1-37}$ and $hIAPP_{8-37}$ oligomerization and fibrillation. Taken together, the ThT binding assay, TEM characterization, NMR spectroscopy, DLS characterization and CD spectroscopy showed that PEG-PE micelles inhibited $hIAPP_{1-37}$ and $hIAPP_{8-37}$ aggregation through inhibiting the β-sheet structures formation (Figs 1 and 2, Supplementary Figure S1, and Supplementary Tables S1, S2). Since PEG-PE micelles have amphiphilic nano-cages that consist of hydrophilic PEG chain and hydrophobic PE core as previously reported[21], we hypothesized that PEG-PE micelles could effectively prevent $hIAPP_{1-37}$ and $hIAPP_{8-37}$ aggregation by capturing $hIAPP_{1-37}$ and $hIAPP_{8-37}$ monomers and its intermediate oligomeric aggregates into their nano-cages. In order to verify the hypothesis, the time-resolved dot blot assay was exploited to measure the formation of $hIAPP_{1-37}$ and $hIAPP_{8-37}$ oligomers and fibrils in the absence and presence of PEG-PE micelles. $hIAPP_{1-37}$ and $hIAPP_{8-37}$ were incubated in the absence and presence of tenfold excess amount of PEG-PE micelles for 24 h, and the abundance of both oligomers and fibrils at different time intervals were determined using anti-oligomer (A11) and anti-amyloid fibrils polyclonal antibodies[30,31]. As shown in Fig. 3, dot blot assay revealed that the amount of $hIAPP_{1-37}$ and $hIAPP_{8-37}$ oligomers and fibrils increased in a time-dependent manner in the absence of PEG-PE micelles, while significantly decreased in the presence of PEG-PE micelles and remained less over 24 h of incubation at 37 °C.

The effect of PEG-PE micelles on $hIAPP_{1-37}$ and $hIAPP_{8-37}$ induced-cytotoxicity. Since hIAPP aggregation is associated with the pathogenesis of T2DM[3,4,9], we hypothesized that PEG-PE micelles that effectively inhibited the oligomerization and fibrillation of $hIAPP_{1-37}$ and $hIAPP_{8-37}$ might reduce the cytotoxicity mediated by $hIAPP_{1-37}$ and $hIAPP_{8-37}$. In this study, INS-1 cell line was used as a pancreatic β-cell model system to evaluate the effect of PEG-PE micelles on $hIAPP_{1-37}$- and $hIAPP_{8-37}$-induced cytotoxicity. The negligible cytotoxicity induced by PEG-PE itself with varying concentrations from 1 μM to 60 μM was observed (cell viability > 95%), suggesting the great biocompatibility of PEG-PE (Supplementary Figure S2). Taking the cytotoxicity issue into consideration, we used PEG-PE concentration under 60 μM for the following cell experiments. INS-1 cells were incubated with $hIAPP_{1-37}$ (1–20 μM) and $hIAPP_{8-37}$ (1–20 μM) in the absence and presence of PEG-PE micelles (20 μM) for 48 h. MTS assay was performed to determine the cell viability. We found that the viabilities of both $hIAPP_{1-37}$- and $hIAPP_{8-37}$-treated cells in the absence of PEG-PE micelles were gradually decreased when the concentrations of $hIAPP_{1-37}$ and $hIAPP_{8-37}$ were increased from 1 μM to 20 μM (Fig. 4a,b), indicating the cytotoxicity induced by hIAPP. PEG-PE micelle alone is nearly non-toxic (Supplementary Figure S2) and can significantly reduce the toxicity of $hIAPP_{1-37}$ (Fig. 4a) and $hIAPP_{8-37}$ (Fig. 4b) by decreasing the amount of hIAPP oligomers and fibrils.

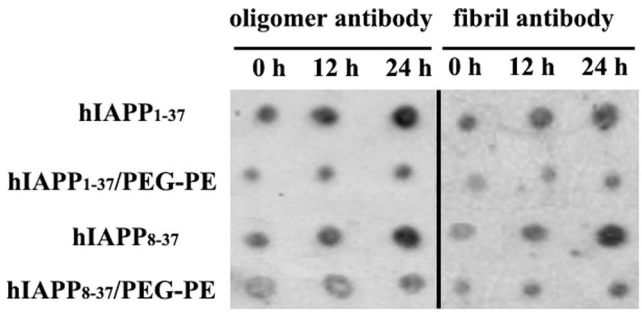

Figure 3. The effect of PEG-PE micelles on $hIAPP_{1-37}$ and $hIAPP_{8-37}$ oligomerization and fibrillation. Dot blots of 20 μM solutions of $hIAPP_{1-37}$ and $hIAPP_{8-37}$ were aged for 0, 12, 24 h in the absence and presence of 200 μM of PEG-PE micelles, spotted onto the nitrocellulose membranes, and probed with the anti-oligomer polyclonal antibody (A11). The same membranes of $hIAPP_{1-37}$ and $hIAPP_{8-37}$ in the absence and presence of 200 μM of PEG-PE micelles were also immunostained with the anti-amyloid fibrils polyclonal antibody.

It has been generally accepted that amyloid oligomers have greater cytotoxicity due to their higher membrane permeability as compared to monomers and mature fibrils[32,33]. The amyloid oligomer-induced membrane permeability, which leads to the cell dysfunction and cell death, can be inhibited by the anti-oligomer antibody[34] or amyloid aggregation inhibitors[35]. In addition to the cell membrane permeability, a large number of studies have demonstrated that the generation of reactive oxygen species (ROS) during oxidative stress is also strongly linked to pancreatic β-cell death[36]. Treatment of β-cells with exogenous hIAPP resulted in intracellular ROS accumulation, and treatment with antioxidant inhibited the progression of hIAPP-induced β-cell death[37]. In order to clarify the underlying molecular mechanisms of inhibition of hIAPP-mediated β-cell death by PEG-PE micelle, we therefore evaluated the effect of PEG-PE micelles on $hIAPP_{1-37}$- and $hIAPP_{8-37}$-induced cell membrane permeability and oxidative stress. INS-1 cells were incubated with $hIAPP_{1-37}$ (1–20 μM) and $hIAPP_{8-37}$ (1–20 μM) in the absence and presence of PEG-PE micelles (20 μM) for 24 h. The results showed that the amount of released lactate dehydrogenase (LDH) was increased when the concentrations of $hIAPP_{1-37}$ and $hIAPP_{8-37}$ were increased from 1 μM to 20 μM in the absence of PEG-PE micelles (Fig. 4c,d), confirming the $hIAPP_{1-37}$- and $hIAPP_{8-37}$-induced cell membrane permeability. However, the amount of released LDH that induced by $hIAPP_{1-37}$ and $hIAPP_{8-37}$ in the presence of PEG-PE micelles is significantly decreased compared to $hIAPP_{1-37}$ and $hIAPP_{8-37}$ alone (Fig. 4c,d). Meanwhile, intracellular ROS was measured by a fluorescein-labeled dye DCFH-DA. Treatment with $hIAPP_{1-37}$ and $hIAPP_{8-37}$ alone increased the intracellular ROS level of INS-1 cells in a dose-dependent manner (Fig. 4e,f), confirming that the oxidative stress was also responsible for $hIAPP_{1-37}$- and $hIAPP_{8-37}$-induced cell death, which was consistent with the previous report[36,37]. In contrast, declined ROS level in $hIAPP_{8-37}$-treated cells because of the addition of PEG-PE micelles was observed, suggesting that PEG-PE micelles effectively rescued $hIAPP_{8-37}$-induced INS-1 cell death through alleviating the oxidative stress (Fig. 4f). Taken together, these results demonstrated that both the cell membrane permeability and the oxidative stress play central roles in hIAPP-mediated β-cell death. PEG-PE micelles were demonstrated to inhibit $hIAPP_{1-37}$ and $hIAPP_{8-37}$ oligomerization and fibrillation and to rescue $hIAPP_{1-37}$- and $hIAPP_{8-37}$-induced cytotoxicity. PEG-PE micelles reduced the cytotoxicity by decreasing the cell membrane permeability and alleviating the oxidative stress.

PEG-PE micelles can remodel the preformed $hIAPP_{1-37}$ and $hIAPP_{8-37}$ fibrils and rescue fibrils-mediated cytotoxicity to INS-1 cells. Since the extracellular aggregation of hIAPP and the fibrils extension can cause the invagination and perforation of cell membranes[36], inhibitors that have an ability to remodel the preformed mature fibrils are desired for rescuing mature fibrils-mediated cytotoxicity. In our previous work, we have demonstrated that, in the presence of DTT, PEG-PE micelles not only prevented insulin aggregation but also remodelled the preformed insulin aggregates[20]. Therefore, we further investigated whether this property of PEG-PE micelles is applicable to the preformed hIAPP fibrils. 20 μM solutions of $hIAPP_{1-37}$ and $hIAPP_{8-37}$ were aged for 24 h at 37 °C to form fibrils and then exposed to the increasing concentrations of PEG-PE micelles for a further 96 h. The aged $hIAPP_{1-37}$ and $hIAPP_{8-37}$ fibrils in the absence of PEG-PE micelles exhibited a pronounced ThT signal, but the addition of PEG-PE micelles reduced the signal in a dose-dependent manner (Fig. 5a,b). PEG-PE micelles concentration higher than/or equal to stoichiometric ratio can effectively remodel hIAPP fibril. Results indicated that PEG-PE micelles actively remodelled the relatively stable 1:1 co-aggregates formation through reacting with monomers or small oligomers of $hIAPP_{1-37}$ and $hIAPP_{8-37}$. PEG-PE micelles shifted the $hIAPP_{1-37}$ and $hIAPP_{8-37}$ aggregation equilibrium toward monomers and small oligomers, which allowed the assembly of these co-aggregates. Furthermore, we determined the conformational changes of the aged samples of $hIAPP_{1-37}$ and $hIAPP_{8-37}$ using CD spectra, samples were incubated with and without PEG-PE micelles for an additional 96 h before analysis. $hIAPP_{1-37}$ and $hIAPP_{8-37}$ fibrils mainly adopted a predominant β-sheet structures in the absence of PEG-PE micelles (Fig. 5c,d). The secondary structures of $hIAPP_{1-37}$ and $hIAPP_{8-37}$ fibrils were significantly changed from β-sheet into α-helix in the presence of 10-fold and 20-fold excess amount of PEG-PE micelles, which supported the results from ThT binding assay.

The remodelling of fibrillar $hIAPP_{1-37}$ and $hIAPP_{8-37}$ by PEG-PE micelles was also confirmed by TEM analysis. Samples of $hIAPP_{1-37}$ and $hIAPP_{8-37}$ fibrils in the absence and presence of PEG-PE micelles were loaded over copper grids directly after CD experiments. Both $hIAPP_{1-37}$ and $hIAPP_{8-37}$ formed long unbranched fibrils

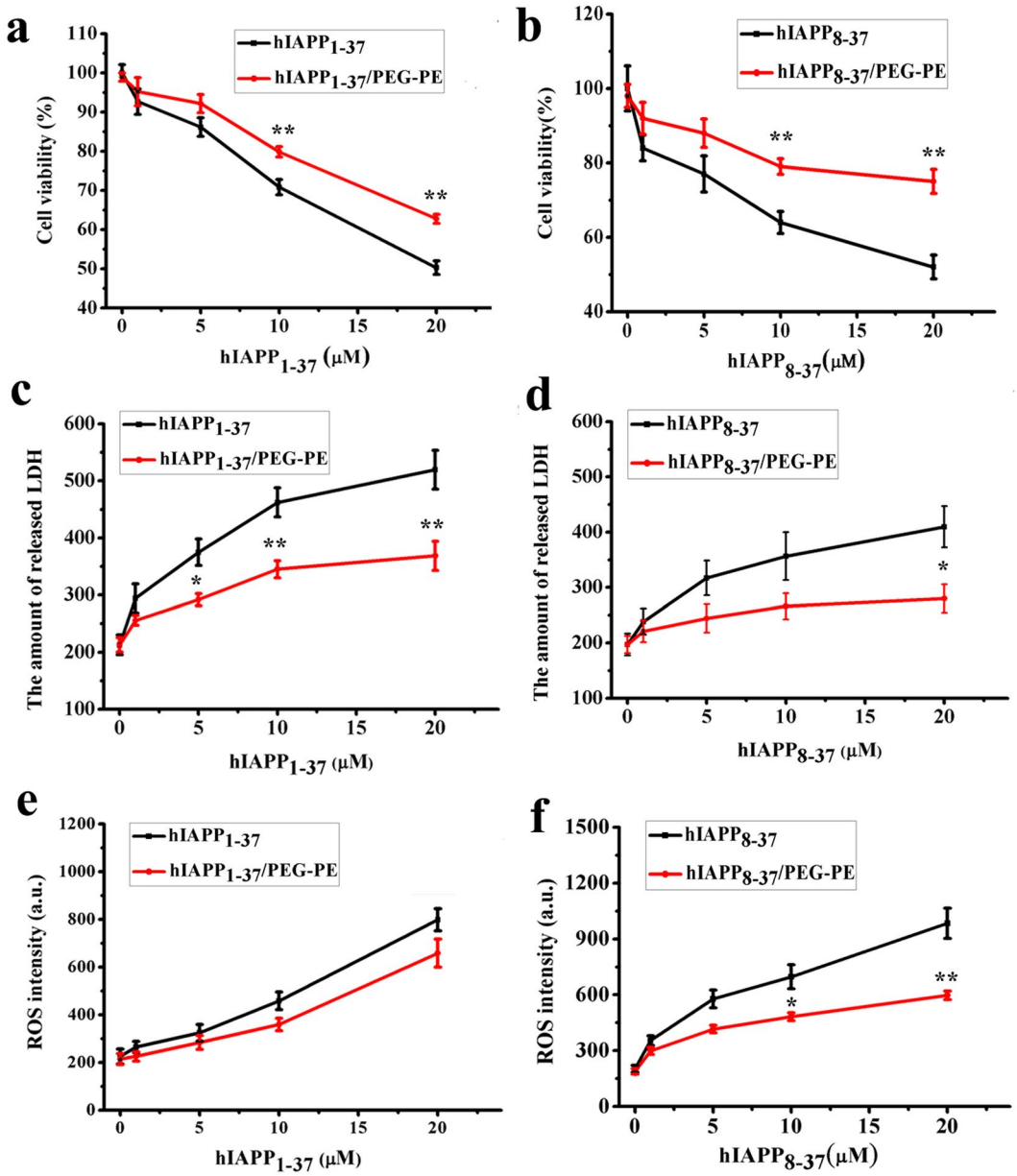

Figure 4. The effect of PEG-PE micelles on $hIAPP_{1-37}$ and $hIAPP_{8-37}$ induced-cytotoxicity. (**a**,**c**,**e**) $hIAPP_{1-37}$ (1 μM, 5 μM, 10 μM, and 20 μM) and (**b**,**d**,**f**) $hIAPP_{8-37}$ (1 μM, 5 μM, 10 μM, and 20 μM) solutions and the mixture of $hIAPP_{1-37}$/PEG-PE (1 μM/20 μM, 5 μM/20 μM, 10 μM/20 μM, and 20 μM/20 μM) and $hIAPP_{8-37}$/PEG-PE (1 μM/20 μM, 5 μM/20 μM, 10 μM/20 μM, and 20 μM/20 μM) were incubated with INS-1 cells for 24 and 48 h at 37 °C. (**a**,**b**) Cell viability was evaluated by the MTS assay. (**c**,**d**) The amount of released LDH in the culture medium was determined by a LDH assay reagent. (**e**,**f**) ROS was determined by measuring the fluorescence intensity of an oxidation-sensitive fluorescein DCFH-DA. Significance ($*p < 0.05$ and $**p < 0.01$) was calculated relative to $hIAPP_{1-37}$ and $hIAPP_{8-37}$, respectively. Error bars represent standard deviation ($n = 3$).

as they aged, but PEG-PE micelles significantly decreased the amount of $hIAPP_{1-37}$ and $hIAPP_{8-37}$ fibrils in a dose-dependent manner (Fig. 6a,b). Compared with $hIAPP_{1-37}$ and $hIAPP_{8-37}$ fibrils, the average length of fibrils in the presence of PEG-PE micelle was shortened, but the average width of fibrils did not change.

The remodelling of $hIAPP_{1-37}$ and $hIAPP_{8-37}$ fibrils by PEG-PE micelles could possibly produce adverse effects *in vivo* if it increases the amount of toxic intermediates, such as amyloid oligomers[32,33]. In order to confirm that the remodelling of hIAPP fibrils does not involve the formation of toxic soluble oligomers, PEG-PE micelles-treated $hIAPP_{1-37}$ and $hIAPP_{8-37}$ fibrils were tested for their reactivity toward the anti-oligomer and anti-amyloid fibril antibodies. The results demonstrated that PEG-PE micelles effectively decreased the amounts of both oligomers and amyloid fibrils of the aged $hIAPP_{1-37}$ and $hIAPP_{8-37}$ samples in a dose-dependent manner (Fig. 6c,d), implying that the remodelling of $hIAPP_{1-37}$ and $hIAPP_{8-37}$ fibrils by PEG-PE micelles led to the formation of co-aggregates that were distinct from soluble oligomers and mature fibrils. Next, we determined whether PEG-PE micelles

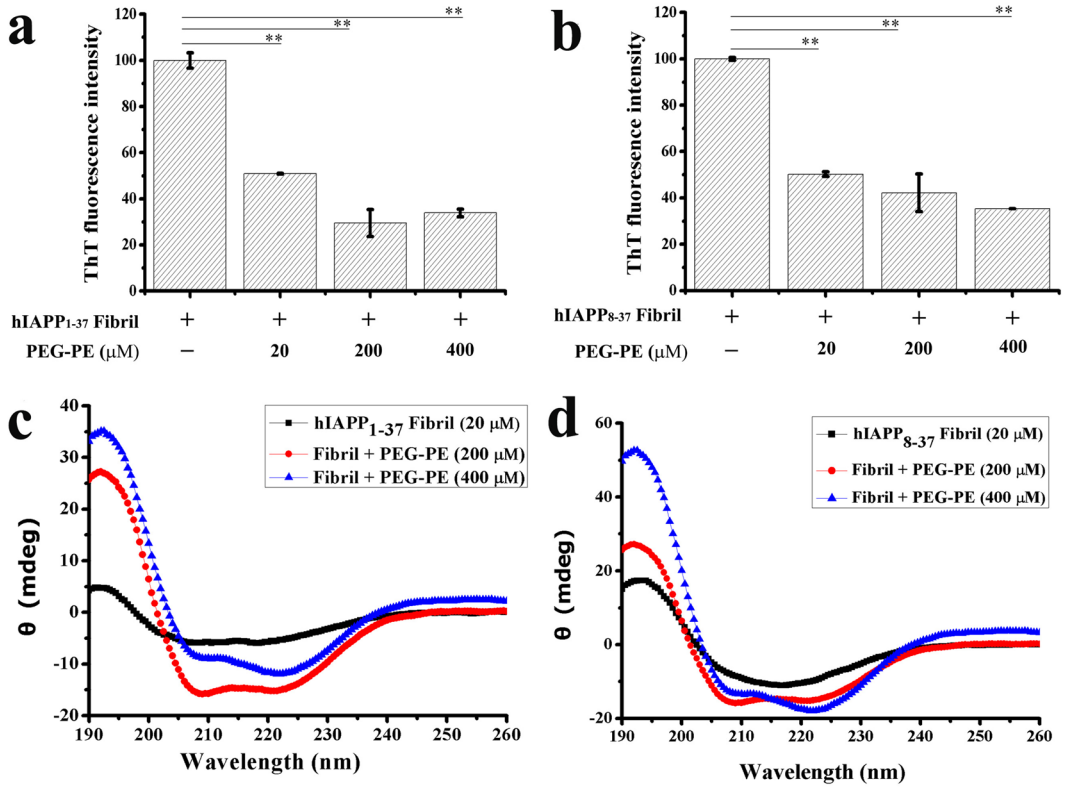

Figure 5. PEG-PE micelles can reverse the conformational transition of $hIAPP_{1-37}$ and $hIAPP_{8-37}$ fibrils from β-sheet to α-helical structures. (**a**,**b**) 20 μM solutions of (**a**) $hIAPP_{1-37}$ and (**b**) $hIAPP_{8-37}$ were aged for 24 h at 37 °C to afford maximal ThT fluorescence. The aged samples were then incubated with freshly prepared PEG-PE micelles (20 μM, 200 μM, and 400 μM) for an additional 96 h and then examined by ThT binding assay. The ThT fluorescence values of aged $hIAPP_{1-37}$ fibril and $hIAPP_{8-37}$ fibril in the absence of PEG-PE micelles were referred to as 100%. Significance ($*p < 0.05$ and $**p < 0.01$) was calculated relative to the $hIAPP_{1-37}$ and $hIAPP_{8-37}$ fibrils, respectively. Error bars represent standard deviation ($n = 3$). (**c**,**d**) CD spectra of (**c**) $hIAPP_{1-37}$ (20 μM) and (**d**) $hIAPP_{8-37}$ (20 μM) were aged for 24 h at 37 °C, and the aged samples were incubated with and without tenfold and twentyfold excess concentrations of PEG-PE micelles for an additional 96 h. The spectra represent the average of six scans after subtracting the contribution of the PEG-PE micelles at identical concentrations.

could reduce hIAPP fibrils-induced cytotoxicity to INS-1 cells. $hIAPP_{1-37}$ and $hIAPP_{8-37}$ fibrils and the mixture of fibrils/PEG-PE were incubated with INS-1 cells for an additional 24 and 48 h. Amount of released LDH and cell viability were evaluated according to the above-mentioned procedures. The results from MTS assay indicated that hIAPP fibrils-induced cytotoxicity was attenuated by PEG-PE micelles dose-dependently (Fig. 7c,d). In accordance with MTS results, declined LDH release due to the addition of PEG-PE micelles further validated the reduced hIAPP fibrils-mediated cytotoxicity (Fig. 7a,b).

As shown in Fig. 8, the soluble monomeric form of hIAPP peptide undergoes specific conformational transitions into aggregation-prone "partially unfolded intermediates" and subsequently aggregates into oligomers. The oligomers serve as templates for further hIAPP deposition, resulting in rapid fibril growth and eventually in the formation of insoluble amyloid fibrils, as previously reported[38]. Although the precise mechanism that how PEG-PE micelle inhibits hIAPP aggregation and remodels the preformed hIAPP fibrils required further research. A plausible mechanism may be proposed that, in the presence of PEG-PE micelles, the partially unfolded state of the monomers and other small intermediate units of $hIAPP_{1-37}$ and $hIAPP_{8-37}$ were encapsulated into the amphiphilic nano-cages of PEG-PE micelles, which led to the formation of hIAPP/PEG-PE complexes (co-aggregates). This process could block active sites hidden in the hIAPP amyloidogenic domain that is responsible for its aggregation. Meanwhile, the hydrophilic PEG chains could create a protective barrier layer, which prevents the excessive adsorption of $hIAPP_{1-37}$ and $hIAPP_{8-37}$.

Moreover, the addition of PEG-PE micelles was able to decrease the monomeric concentrations of $hIAPP_{1-37}$ and $hIAPP_{8-37}$ in solution, which disturbed the dynamic equilibrium between monomeric and oligomeric species and shifted the hIAPP aggregation pathway from an "on-pathway" to an "off-pathway" mechanism.

Discussion

Although insulin can temporarily alleviate the conditions of T2DM, but currently there is no effective treatment that can suppress or cure this disease. In addition, evidences from clinical studies suggest that people suffering from T2DM have greater chance of developing AD in comparison to healthy individuals[39], hence researches for new therapeutic strategies for T2DM are still important and in demand. It has been widely recognized that the

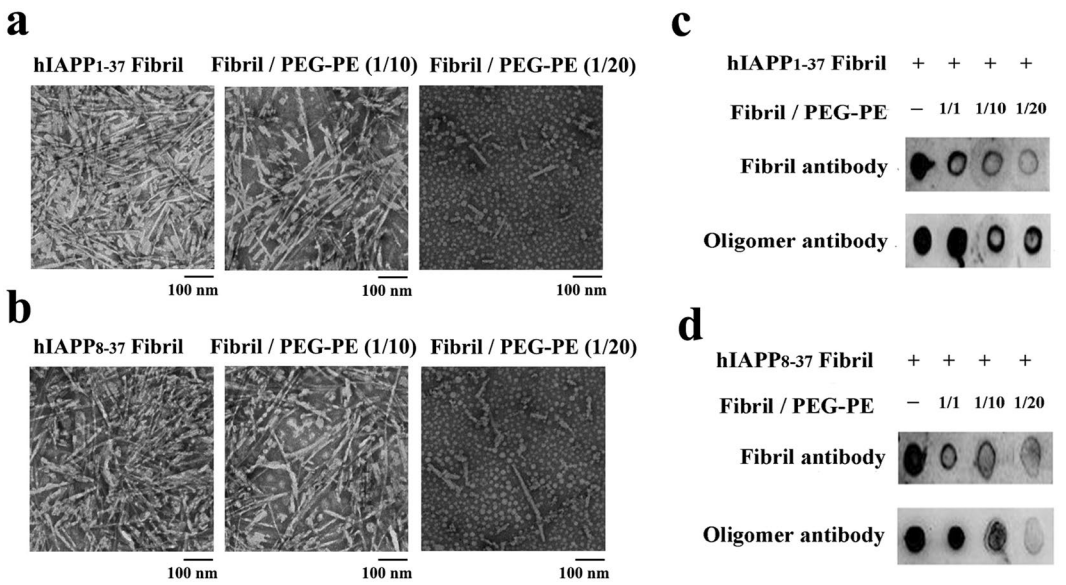

Figure 6. PEG-PE micelles can remodel fibrillar $hIAPP_{1-37}$ and $hIAPP_{8-37}$ into species that are non-reactive toward oligomer- and fibril antibodies. (**a**,**b**) TEM images of (**a**) $hIAPP_{1-37}$ (20 μM) and (**b**) $hIAPP_{8-37}$ (20 μM) were aged for 24 h at 37 °C, and the aged samples were incubated with and without tenfold and twentyfold excess concentrations of PEG-PE micelles for an additional 96 h. (**c**,**d**) Dot blots of 20 μM of (**c**) $hIAPP_{1-37}$ and (**d**) $hIAPP_{8-37}$ were aged for 24 h at 37 °C, and the aged samples were then incubated with and without freshly prepared PEG-PE micelles (20 μM, 200 μM, and 400 μM) for a further 96 h. The disaggregation products were tested by dot blot assay using anti-oligomer and anti-amyloid fibril polyclonal antibodies.

aggregation of monomeric hIAPP into insoluble plaque-associated amyloid fibrils is a crucial step that drives T2DM pathogenesis[4,38]. Based on this hypothesis regarding amyloids, extensive efforts have been dedicated to developing hIAPP inhibitors[11–18]. Among developed hIAPP inhibitors, nanomaterials have been drawing great attention due to their small size and physicochemical properties, especially their partial hydrophobicity. This property of nanomaterials allows them to pass through cell membranes and enter different cells and organelles, perturbing self-assembly pathways of proteins[15]. Either inhibitory or enhancement effect on the process of amyloid aggregation have been reported, while the application of the nanomaterials in remodelling amyloid aggregation is quite limited due to their biocompatibility issues[40,41]. Therefore, it is necessary and of great significance to develop nanomaterials with good safety and biocompatibility as a novel hIAPP inhibitor, so that more therapeutic options can be provided to the patients.

In this work, we demonstrated that self-assembled PEG-PE micelles effectively rescued $hIAPP_{1-37}$- and $hIAPP_{8-37}$-induced cytotoxicity through either inhibiting $hIAPP_{1-37}$ and $hIAPP_{8-37}$ oligomerization and fibrillation or remodelling the preformed $hIAPP_{1-37}$ and $hIAPP_{8-37}$ fibrils. PEG-PE copolymer that consists of hydrophilic PEG and hydrophobic PE is ideal for forming micelles, and PEG-PE micelles have a low CMC (~10 μM) and small size distribution (~15-20 nm)[19]. Moreover, PEG-PE micelles show superior biocompatibility as they were approved by the Food and Drug Administration (FDA) as a pharmaceutical excipient for Doxil® (liposomal formulation of doxorubicin)[42].

In this study, the inhibitory effects of PEG-PE micelles on $hIAPP_{1-37}$ and $hIAPP_{8-37}$ are very similar. There are two possible reasons to explain this phenomenon. One reason could be related to the isoelectric points (PI) of $hIAPP_{1-37}$ (PI:8.9), $hIAPP_{8-37}$ (PI:8.8) and PEG-PE polymer (PI:5.93). At pH 7.4, This PEG-PE polymer is negatively charged due to the de-protonation of the phosphate group that exists between hydrophilic PEG and hydrophobic PE. Both $hIAPP_{1-37}$ and $hIAPP_{8-37}$ are positively charged, and they have almost the same charge due to their similar PI. The electrostatic interactions between these two peptides and PEG-PE micelles may play critical roles in hIAPP encapsulation, which inhibited hIAPP aggregation. The other reason is that the first 7 amino acids have neglectable impact on the aggregation of hIAPP. The β-hairpin structure of hIAPP has been obtained by solid-state NMR, suggesting the parallel β-sheet structures with 10 residues in the core domains[43]. The fragment $IAPP_{1-7}$ is believed to be non-β-sheet structure as the result of the disulfide bond between cysteine residues 2 and 7[44]. Thus these two peptides have similarity in β-sheet structures and also aggregation propensity.

Extensive studies have shown that the imbalance between hIAPP anabolism and catabolism in the pancreatic islet is the primary event responsible for the pathogenesis of T2DM[38]. In healthy individuals, the production of hIAPP is normally in equilibrium with its excretion from body. Both overproduction and imbalance in excretion from body could disrupt hIAPP homeostasis, which leads to dysfunction and death of pancreatic β-cell due to the generation of hIAPP amyloid aggregates with variable cytotoxicity. From preceding results it is proved that PEG-PE micelles possess capability to maintain hIAPP homeostasis by simultaneously inhibiting hIAPP aggregation and promoting disaggregation of hIAPP aggregates that eventually diminished hIAPP-mediated cytotoxicity. In conclusion, this study may provide an attractive therapeutic strategy for generating a PEG-PE micelle-based anti-diabetic agent that will help to develop new drugs for T2DM therapy.

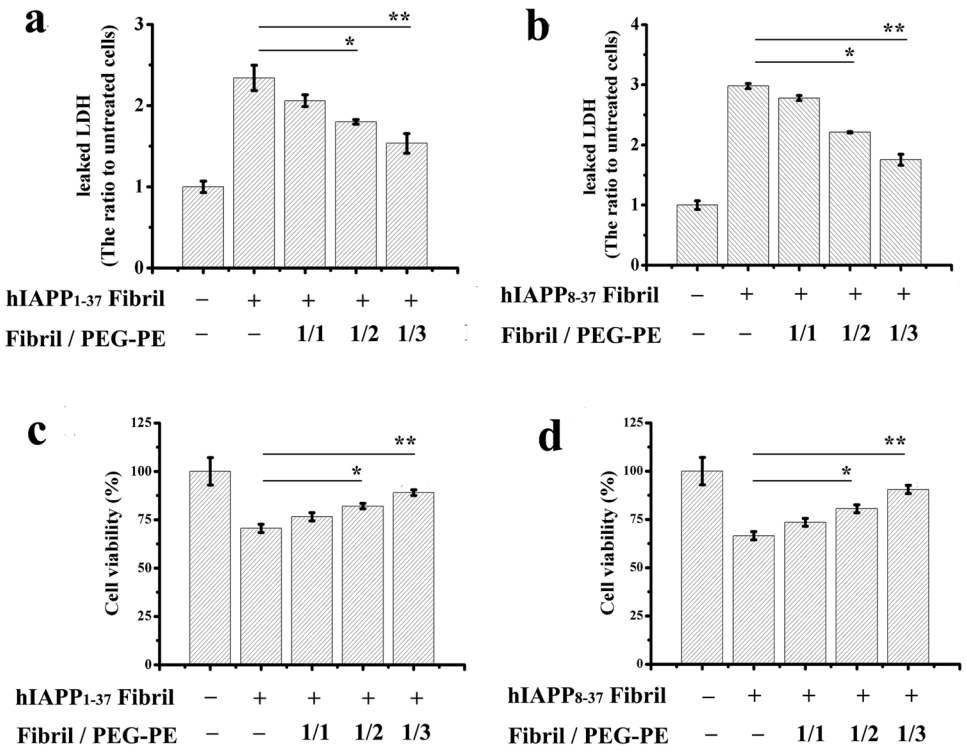

Figure 7. Dose-dependent effect of PEG-PE micelles on the $hIAPP_{1-37}$ and $hIAPP_{8-37}$ fibrils-mediated cytotoxicity to INS-1 cells. (**a**,**c**) $hIAPP_{1-37}$ (20 μM) and (**b**,**d**) $hIAPP_{8-37}$ (20 μM) were aged for 24 h at 37 °C, and the aged samples were then incubated for a further 96 h in the absence and presence of increasing concentrations of PEG-PE micelles (20 μM, 40 μM, and 60 μM). $hIAPP_{1-37}$ and $hIAPP_{8-37}$ fibrils and the mixture of fibril/PEG-PE were exposed to INS-1 cells for an additional 24 and 48 h. (**a**,**b**) The amount of released LDH in the culture medium was determined by a LDH assay reagent. (**c**,**d**) The cell viability was measured by the MTS assay. Results were expressed as a percentage of the control group and were reported as mean ± standard deviation (SD) from three assays. Significance ($*p < 0.05$ and $**p < 0.01$) was calculated relative to the $hIAPP_{1-37}$ and $hIAPP_{8-37}$ fibrils, respectively.

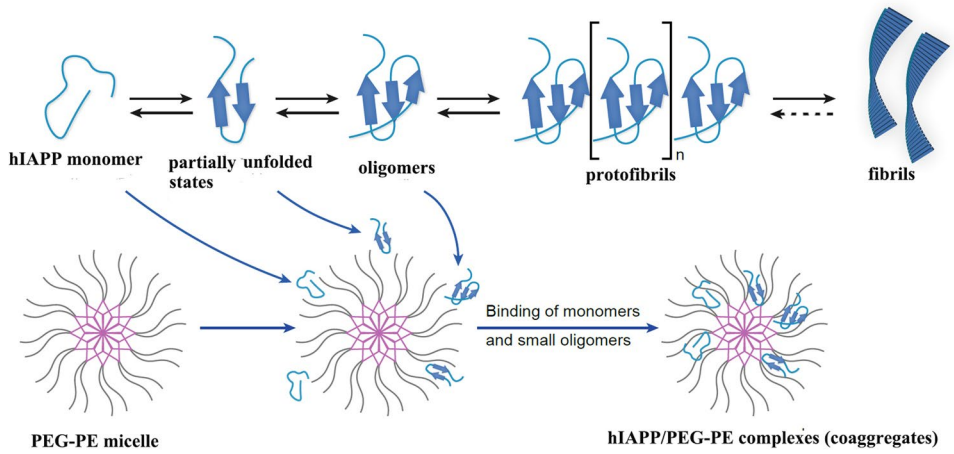

Figure 8. Schematic illustration of the possible mechanism of the interaction between PEG-PE micelles and hIAPP on the kinetics of amyloid fibrillation process.

Methods

Chemicals and materials. Lyophilized powders of $hIAPP_{1-37}$ and $hIAPP_{8-37}$ were purchased from GL Biochem Ltd. (Shanghai, China), and the purity of peptides (>98%) has been verified by high performance liquid chromatography (HPLC) and mass spectrum (MS). Distearoyl-*sn*-glycero-3-phosphoethanolamine-*n*-[methoxy (polyethylene glycol)-2000] (PEG-PE) was purchased from Avanti Polar Lipids (Alabaster, AL). INS-1 cell line

was purchased from Chinese Academy of Medical Science & Peking Union Medical College, Beijing, China. All other chemicals were of analytical grade and used without any further purification.

hIAPP and hIAPP/PEG-PE preparation. $hIAPP_{1-37}$ and $hIAPP_{8-37}$ preparations were prepared according to the previously published protocol with modification[28]. Briefly, $hIAPP_{1-37}$ and $hIAPP_{8-37}$ were dissolved in HFIP to the final concentration of 1 mM and aliquoted in microcentrifuge tubes. The solutions were sonicated in a water bath for 10 min and centrifuged at 4 °C for 10 min. The supernatants of $hIAPP_{1-37}$ and $hIAPP_{8-37}$ were collected and stored at −80 °C. Prior to use, HFIP was evaporated by vacuum rotary evaporator, and $hIAPP_{1-37}$ and $hIAPP_{8-37}$ solutions were prepared by dissolving with PBS and ddH_2O using DMSO as a hydrotropic agent. On the other hand, $hIAPP_{1-37}$ and $hIAPP_{8-37}$ encapsulated into PEG-PE micelles were prepared via the film dispersion method, as previously described[19]. Firstly, the supernatant of $hIAPP_{1-37}$ and $hIAPP_{8-37}$ solutions in HFIP was mixed with a PEG-PE solution in chloroform at different molar ratios of 1:1~20 (hIAPP:PEG-PE) at room temperature. Secondly, the organic solvent of the mixed solution was evaporated by vacuum rotary evaporator to form a dry lipid film. Finally, the lipid film was rehydrated with PBS and ddH_2O to obtain the $hIAPP_{1-37}$ and $hIAPP_{8-37}$ encapsulated into PEG-PE micelles ($hIAPP_{1-37}$/PEG-PE and $hIAPP_{8-37}$/PEG-PE).

ThT binding assay. The extent of $hIAPP_{1-37}$ and $hIAPP_{8-37}$ aggregation in the absence and presence of PEG-PE micelle was determined using ThT (a fluorescent dye that specifically binds with the β-sheet of amyloid structures[24]). $hIAPP_{1-37}$ and $hIAPP_{8-37}$ solutions (20 μM in PBS) and the mixture of $hIAPP_{1-37}$/PEG-PE and $hIAPP_{8-37}$/PEG-PE (20 μM/20 μM, and 20 μM/200 μM) were added into the wells of 96-well plates. Each sample has three replicated wells and each well contains 20 μM ThT. The plates were covered with Platemax CyclerSeal sealing film (Axygen, USA) and incubated at 37 °C for 2 h to follow hIAPP aggregation dynamics. The fluorescence intensity of each well was measured by spectrophotometer (SpectraMax i3, Molecular Devices, USA) at the excitation and emission wavelengths of 450 and 482 nm, respectively.

TEM characterization. 20 μM solutions of $hIAPP_{1-37}$ and $hIAPP_{8-37}$ in ddH_2O in the absence and presence of 20 μM and 200 μM PEG-PE micelles were incubated for 24 h at 37 °C. 10 μL of each sample was dropped over the copper grid and allowed to adsorb for 10 min at room temperature. After that, the excessive solution was removed from the copper grid by the filter paper. Samples were stained with 1% uranyl acetate for 1 min and washed three times with ddH_2O. TEM measurements were performed with HITACHI TEM (Hitachi, Ltd., Tokyo, Japan) with 80 kV accelerated voltage.

NMR Spectroscopy. PEG-PE stock solution (10 mM) was prepared by dissolving the powder in deuterium oxide. $hIAPP_{1-37}$ stock solution (1 mM) was prepared by dissolving the powder in deuterium oxide using DMSO-d6 as a hydrotropic agent. $hIAPP_{1-37}$ encapsulated into PEG-PE micelles ($hIAPP_{1-37}$/PEG-PE, $hIAPP_{1-37}$: PEG-PE = 1:10, molar ratio) were prepared via the film dispersion method, and the lipid film was rehydrated with deuterium oxide. All NMR spectra were acquired at 298 K with Bruker DPX 400 spectrometer equipped with a Z-gradient BBO probe. The ^1H NMR experiments were performed on the samples containing 0.5 mM $hIAPP_{1-37}$ or 5 mM PEG-PE in D_2O.

DLS characterization. 20 μM solutions of $hIAPP_{1-37}$ and $hIAPP_{8-37}$ in ddH_2O in the absence and presence of 20 μM and 200 μM PEG-PE micelles were incubated for 24 h at 37 °C.

Particle size distribution of each sample was determined by DLS analysis using Nano Particle Analyzer (Malvern Instrument Ltd, Malvern, UK).

CD spectroscopy. CD measurements were performed using Jasco-J810 spectrometer (Jasco, Tokyo, Japan) under a constant flow of nitrogen gas. Freshly prepared solutions of $hIAPP_{1-37}$ and $hIAPP_{8-37}$ in PBS (20 μM) were incubated and analyzed in the absence and presence of 20 μM and 200 μM PEG-PE micelles for 20 min, 2 h and 24 h. Measurements were performed at room temperature in a fused quartz cuvette (1-mm path length). CD spectra were recorded in the range of 190 to 260 nm with a step size and a bandwidth of 1 nm. For each CD measurement, 6 runs were averaged and corrected by subtracting the contribution of the PEG-PE at identical concentrations.

Dot Blot assay. Freshly prepared solutions of $hIAPP_{1-37}$ and $hIAPP_{8-37}$ (20 μM) were incubated at 37 °C for over 24 h in the absence and presence of PEG-PE micelles (200 μM). Samples were collected at 0, 12, 24 h time intervals, respectively. Later on 10 μL of each sample was dropped over a nitrocellulose membrane (0.22 μm) and dried at room temperature. The membrane was blocked with 5% (w/v) nonfat milk in tris-buffered saline containing 0.1% Tween 20 (TBST) for 1 h at room temperature. After being washed with TBST for three times, the membrane was incubated with the anti-oligomer polyclonal antibody (A11) and anti-amyloid fibrils polyclonal antibody at 1:1000 dilution in 5% (w/v) nonfat milk in TBST overnight at 4 °C. Then the membrane was incubated with horseradish peroxidase (HRP) conjugated anti-rabbit IgG at 1:1000 dilution in 5% (w/v) nonfat milk in TBST for 1 h at room temperature. After being washed with TBST for three times, the membrane was developed with enhanced chemiluminescence system.

Cell viability assay. The cell viability was measured using the CellTiter 96® Aqueous One Solution Cell Proliferation assay (also termed as MTS assay, Promega, Madison, Wisconsin, USA). INS-1 cells were plated at 8,000 cells per well in the 96-well plates and were grown overnight before replacing the medium with freshly prepared $hIAPP_{1-37}$ and $hIAPP_{8-37}$ solutions (1 μM, 5 μM, 10 μM, and 20 μM) and with the mixture of $hIAPP_{1-37}$/PEG-PE and $hIAPP_{8-37}$/PEG-PE (1 μM/20 μM, 5 μM/20 μM, 10 μM/20 μM, and 20 μM/20 μM). After 48 h, 20 μL of MTS reagent was added to each well followed by incubation for another 2 h at 37 °C. The absorbance was

measured at 490 nm using spectrophotometer. Wells with culture medium alone (no cells) served as blank controls, and the value of the control cells that treated with same volume of corresponding solution in the absence of hIAPP/PEG-PE was set as 100%.

LDH assay. The release of LDH indicates the change of cell membrane permeability, which can reflect the extent of cell membranes damage[45]. INS-1 cells were plated at 8,000 cells per well in the 96-well plates and were grown overnight. Later on, cell were treated with freshly prepared $hIAPP_{1-37}$ and $hIAPP_{8-37}$ solutions (1 μM, 5 μM, 10 μM, and 20 μM) in the absence and presence of PEG-PE micelles (20 μM) followed by incubation for 24 h at 37 °C. After 24 h, the cell culture medium was transferred to a new 96-well plate followed by the addition of 50 μL of LDH assay reagent (Promega, Madison, Wisconsin, USA) into each well. Later on, cells were incubated in the dark for 30 min at room temperature, and the absorbance of each well was measured at 490 nm using spectrophotometer. The control cells were treated with same volume of corresponding solution in the absence of hIAPP/PEG-PE.

ROS assay. 50,000 cells/well were plated in 24-well plates and cultured overnight. Later on cells were exposed to freshly prepared $hIAPP_{1-37}$ and $hIAPP_{8-37}$ solutions (1 μM, 5 μM, 10 μM, and 20 μM) and to the mixture of $hIAPP_{1-37}$/PEG-PE and $hIAPP_{8-37}$/PEG-PE (1 μM/20 μM, 5 μM/20 μM, 10 μM/20 μM, and 20 μM/20 μM) followed by incubation for an additional 24 h at 37 °C. After incubation period of 24 h, cell culture medium of each well was replaced with 1 mL fresh medium containing 1 μL of ROS probe DCFH-DA (10 mM). After 20 min of incubation at 37 °C with DCFH-DA, 1×10^4 cells were collected and subjected to Accuri™ C6 flow cytometer (BD Biosciences, San Jose, CA), acquired data was analysed with CellQuest software.

Fibrils remodelling assay. $hIAPP_{1-37}$ and $hIAPP_{8-37}$ solutions were incubated in ddH_2O for 24 h at 37 °C to produce $hIAPP_{1-37}$ and $hIAPP_{8-37}$ fibrils. Later on, the aged $hIAPP_{1-37}$ and $hIAPP_{8-37}$ fibrils were mixed with PEG-PE micelles at different molar ratios from 1:1 to 20:1 (PEG-PE: Fibril) followed by incubation for an additional 96 h at 37 °C. The ThT binding assay, CD spectroscopy, TEM, dot blot assay, LDH assay and cell viability assay of $hIAPP_{1-37}$ and $hIAPP_{8-37}$ fibrils in the absence and presence of PEG-PE micelles were performed according to the above-mentioned experimental procedure.

Statistical analysis. All experiments were carried out at least three times with three independent samples. Data were expressed as means ± SD unless noted otherwise. Unpaired Student's t-test was performed to assess the statistical significance of the results and was expressed in terms of *p* values, *p* value less than 0.05 are indicated by * and *p* value less than 0.01 are indicated by **.

References

1. Mattson, M. P. Pathways towards and away from Alzheimer's disease. *Nature* **430**, 631–639 (2004).
2. Selkoe, D. J. Folding proteins in fatal ways. *Nature* **426**, 900–904 (2003).
3. Sipe, J. D. *et al*. Nomenclature 2014: Amyloid fibril proteins and clinical classification of the amyloidosis. *Amyloid* **21**, 221–224 (2014).
4. Verchere, C. B. *et al*. Islet amyloid formation associated with hyperglycemia in transgenic mice with pancreatic beta cell expression of human islet amyloid polypeptide. *P. Natl. Acad. Sci. USA* **93**, 3492–3496 (1996).
5. Goldsbury, C. *et al*. Amyloid fibril formation from full-length and fragments of amylin. *J. Struct. Biol.* **130**, 352–362 (2000).
6. Konarkowska, B., Aitken, J. F., Kistler, J., Zhang, S. & Cooper, G. J. The aggregation potential of human amylin determines its cytotoxicity towards islet beta-cells. *FEBS J.* **273**, 3614–3624 (2006).
7. Höppener, J. W., Ahrén, B. & Lips, C. J. Islet amyloid and type 2 diabetes mellitus. *New Engl. J. Med.* **343**, 411–419 (2000).
8. Cooper, G. J., Willis, A. C. & Leighton, B. Amylin hormone. *Nature* **340**, 272 (1989).
9. Opie, E. L. The relation of diabetes mellitus to lesions of the pancreas. *Hyaline degeneration of the islands of langerhans. J. Exp. Med.* **5**, 527–540 (1901).
10. Novials, A., Sarri, Y., Casamitjana, R., Rivera, F. & Gomis, R. Regulation of islet amyloid polypeptide in human pancreatic islets. *Diabetes* **42**, 1514–1519 (1993).
11. Scrocchi, L. A. *et al*. Design of peptide-based inhibitors of human islet amyloid polypeptide fibrillogenesis. *J. Mol. Biol.* **318**, 697–706 (2002).
12. Lee, T. Y. *et al*. A Co(III) complex cleaving soluble oligomers of h-IAPP in the presence of polymeric aggregates of h-IAPP. *Bioorg. Med. Chem. Lett.* **22**, 5689–5693 (2012).
13. Jeong, K., Chung, W. Y., Kye, Y. S. & Kim, D. Cu(II) cyclen cleavage agent for human islet amyloid peptide. *Bioorg. Med. Chem.* **18**, 2598–2601 (2010).
14. Mishra, R. *et al*. Small-molecule inhibitors of islet amyloid polypeptide fibril formation. *Angew. Chem. Int. Ed.* **47**, 4679–4682 (2008).
15. Zheng, J. *et al*. Exploring the influence of carbon nanoparticles on the formation of β-sheet-rich oligomers of IAPP22–28 peptide by molecular dynamics simulation. *PLoS ONE* **8**, e65579 (2013).
16. Gurzov, E. N. *et al*. Inhibition of hIAPP amyloid aggregation and pancreatic β-cell toxicity by OH-terminated PAMAM dendrimer. *Small* **12**, 1615–1626 (2016).
17. Klementieva, O. *et al*. Effect of poly(propylene imine) glycodendrimers on β-amyloid aggregation *in vitro* and in APP/PS1 transgenic mice, as a model of brain amyloid deposition and Alzheimer's disease. *Biomacromolecules* **14**, 3570-3580 (2013).
18. Seeliger, J., Werkmüller, A. & Winter, R. Macromolecular crowding as a suppressor of human IAPP fibril formation and cytotoxicity. *PLoS ONE* **8**, e69652 (2013).
19. Tang, N. *et al*. Improving penetration in tumors with nanoassemblies of phospholipids and doxorubicin. *J. Natl. Cancer Inst.* **99**, 1004–1015 (2007).
20. Fang, X. *et al*. Nano-cage-mediated refolding of insulin by PEG-PE micelle. *Biomaterials* **77**, 139–148 (2016).
21. Wang, J. *et al*. Cationic amphiphilic drugs self-assemble to the core-shell interface of PEGylated phospholipid micelles and stabilize micellar structure. *Philos. T. Roy. Soc. A.* **371**, 20120309 (2013).
22. Wang, J., Wang, Y. & Liang, W. Delivery of drugs to cell membranes by encapsulation in PEG-PE micelles. *J. Control Release* **160**, 637–651 (2012).
23. Wang, J., Fang, X. & Liang, W. Pegylated phospholipid micelles induce endoplasmic reticulum-dependent apoptosis of cancer cells but not normal cells. *Acs Nano* **6**, 5018–5130 (2012).

24. Stryer, L. The interaction of napthalene dye with apomyoglobin and apohemoglobin. A fluorescent probe of non-polar binding sites. *J. Mol. Biol.* **13**, 482–495 (1965).
25. Brange, J., Andersen, L., Laursen, E. D., Meyn, G. & Rasmussen, E. Toward understanding insulin fibrillation. *J. Pharm. Sci.* **86**, 517–525 (1997).
26. Li, X., Ma, L., Zheng, W. & Chen, T. Inhibition of islet amyloid polypeptide fibril formation by selenium-containing phycocyanin and prevention of beta cell apoptosis. *Biomaterials* **35**, 8596–8604 (2014).
27. Aitken, J. F. *et al.* Rutin suppresses human-amylin/hIAPP misfolding and oligomer formation *in-vitro*, and ameliorates diabetes and its impacts in human-amylin/hIAPP transgenic mice. *Biochem. Bioph. Res. Co.* **482**, 625–631 (2017).
28. Mao, X. *et al.* Structural characteristics of the beta-sheet-like human and rat islet amyloid polypeptides as determined by scanning tunneling microscopy. *J. Struct. Biol.* **167**, 209–215 (2009).
29. Bahramikia, S. & Yazdanparast, R. Inhibition of human islet amyloid polypeptide or amylin aggregation by two manganese-salen derivatives. *Eur. J. Pharmacol.* **707**, 17–25 (2013).
30. Richman, M. *et al. In vitro* and mechanistic studies of an antiamyloidogenic self-assembled cyclic D,L-alpha-peptide architecture. *J. Am. Chem. Soc.* **135**, 3474–3484 (2013).
31. Kayed, R. *et al.* Fibril specific, conformation dependent antibodies recognize a generic epitope common to amyloid fibrils and fibrillar oligomers that is absent in prefibrillar oligomers. *Mol. Neurodegener.* **2**, 18–28 (2007).
32. Bucciantini, M. *et al.* Inherent toxicity of aggregates implies a common mechanism for protein misfolding diseases. *Nature* **416**, 507–511 (2002).
33. Janson, J., Ashley, R. H., Harrison, D., Mcintyre, S. & Butler, P. C. The mechanism of islet amyloid polypeptide toxicity is membrane disruption by intermediate-sized toxic amyloid particles. *Diabetes* **48**, 491–498 (1999).
34. Kayed, R. *et al.* Permeabilization of lipid bilayers is a common conformation-dependent activity of soluble amyloid oligomers in protein misfolding diseases. *J. Biol. Chem.* **279**, 46363–46366 (2004).
35. Qi, W., Zhang, A., Good, T. A. & Fernandez, E. J. Two disaccharides and trimethylamine N-oxide affect Abeta aggregation differently, but all attenuate oligomer-induced membrane permeability. *Biochemistry* **48**, 8908–8919 (2009).
36. Zraika, S. *et al.* Oxidative stress is induced by islet amyloid formation and time-dependently mediates amyloid-induced beta cell apoptosis. *Diabetologia* **52**, 626–635 (2009).
37. Konarkowska, B., Aitken, J. F., Kistler, J., Zhang, S. & Cooper, G. J. Thiol reducing compounds prevent human amylin-evoked cytotoxicity. *FEBS J.* **272**, 4949–4959 (2005).
38. Westermark, P., Andersson, A. & Westermark, G. T. Islet amyloid polypeptide, islet amyloid, and diabetes mellitus. *Physiol. Rev.* **91**, 795–826 (2011).
39. Hu, R., Zhang, M., Chen, H., Jiang, B. & Zheng, J. Cross-seeding interaction between beta-amyloid and human islet amyloid polypeptide. *ACS Chem. Neurosci.* **6**, 1759–1768 (2015).
40. Chan, H. M. *et al.* Effect of surface-functionalized nanoparticles on the elongation phase of beta-amyloid (1-40) fibrillogenesis. *Biomaterials* **33**, 4443–4450 (2012).
41. Nedumpully-Govindan, P. *et al.* Graphene oxide inhibits hIAPP amyloid fibrillation and toxicity in insulin-producing NIT-1 cells. *Phys. Chem. Chem. Phys.* **18**, 94–100 (2016).
42. Barenholz, Y. Doxil®–the first FDA-approved nano-drug: lessons learned. *J. Control Release* **160**, 117–134 (2012).
43. Luca, S., Yau, W., Leapman, R. & Tycko, R. Peptide conformation and supramolecular organization in amylin fibrils: constraints from solid state NMR. *Biochemistry* **46**, 13505–13522 (2007).
44. Jaikaran, E. & Clark, A. Islet amyloid and type 2 diabetes: from molecular misfolding to islet pathophysiology. *Biochim. Biophys. Acta* **1537**, 179–203 (2001).
45. Kepp, O., Galluzzi, L., Lipinski, M., Yuan, J. & Kroemer, G. Cell death assays for drug discovery. *Nat. Rev. Drug Discov.* **10**, 221–237 (2011).

Acknowledgements

This work was financially supported by the Strategic Priority Research Program of Chinese Academy of Sciences (Grant No. XDA09030306 and XDA09040300). All authors thank Hongbo Guo for TEM technical supporting.

Author Contributions

C.W. and Y.Y. designed the experiments. X.F. carried out main experiments, data analysis, prepared figures and discussed all sections of the manuscript with the corresponding authors. M.Y. and Q.H. discussed part sections of the manuscript with the corresponding authors. All authors contributed in scientific planning, discussions and writing of the manuscript.

Additional Information

Supplementary information accompanies this paper at https://doi.org/10.1038/s41598-018-22820-w.

Competing Interests: The authors declare no competing interests.

Publisher's note: Springer Nature remains neutral with regard to jurisdictional claims in published maps and institutional affiliations.